Modeling and control of active and reactive powers of wind energy conversion system in variable speed based on DFIG

F. Senani [*], A. Rahab [†] and H. Benalla

Faculté des Sciences de la Technologie, Université des frères Mentouri
Laboratoire de l'Electrotechnique de Constantine (LEC), Constantine 1
Ain El-Bey, 25000 Constantine, Algérie

(reçu le 10 Novembre 2015 – accepté le 28 Décembre 2015)

Abstract - *This article describes the modeling and control of wind conversion chain system based on DFIG in variable speed. In fact, the aerodynamic and the electrical models of the wind conversion chain are presented and discussed. Also, the adjustment of active and reactive power is opted in order to ensure optimal operation. For this purpose, a vector control method is applied to ensure a decoupling of its electromechanical quantities. These two parts are developed and programmed in Matlab/Simulink. Some simulation results obtained for the variable-speed operation in hypo- and hyper synchronous modes studied to validate the command will be presented and analyzed.*

Résumé – *Cet article décrit la modélisation et le contrôle du système de la chaîne de conversion du vent basé sur la DFIG à une vitesse variable. A vrai dire, les modèles aérodynamiques et électriques de la chaîne de conversion du vent sont présentés et discutés. Aussi, l'ajustement de la puissance active et réactive est choisi afin d'assurer un fonctionnement optimal. Dans ce but, une méthode de vecteur de contrôle est appliquée pour garantir le découplement de ses quantités électromécaniques. Ces deux parties sont développées avec Matlab/Simulink. Certains résultats de simulation obtenus avec des vitesses de fonctionnement variables dans des modes hypo et hyper synchronisés étudiés pour valider les commandes qui seront présentés et analysés.*

Keywords: Wind turbine - DFIG - Vector control – Indirect control of power (PI) - PWM inverter.

1. INTRODUCTION

The wind energy appears clearly at the right place among the renewable energies, not as a replacement in conventional, but as energy of complementary supplement to the other sources such the nuclear energy, the hydropower, the thermal energy.

Today, many research works concern the integration and the impacts of the wind energy on the distribution networks [1, 2]. So, several technologies of wind generators are at present proposed on the market to know:

- The structure with cage induction machine connected directly to the network: simple and strong solution, it is the oldest structure (Fixed speed wind turbines) [3].
- The structure with permanent magnets synchronous machine, connected to the network through an interface of electronics of power size in approximately 100 % of the rated nominal power [3].
- The structure of asynchronous machine Based on doubly-fed induction has a main feature that it consists of a wound-rotor asynchronous machine and it can also provide the active power to the grid through the stator and the rotor. It allows thanks to this structure to obtain a good efficiency over a wide wind speed range.

[*] senani.fouzi@gmail.com
[†] rahababderezzak@gmail.com , benalladz@yahoo.fr

The DFIG is dimensioned so that the power converters in the rotor are crossed only by 30% of the nominal power. It uses consequently the converters undersized and therefore cheaper [2-5]. The inverter connected to the rotor of the DFIG must provide the necessary complement frequency in order to maintain constant the stator frequency despite the variation of the mechanical speed [6].

Several methods for controlling the DFIG appeared, among them, the vector control. The principle of this technique is to direct the flow vector to make this machine similar control standpoint to a DC machine with separate excitation. This command based on conventional controllers (proportional control, integral and derivative) [3-5]

The first part of this article will be dedicated to the modeling of the various parts of the wind system with a DFIG. The second part concerns the strategy of control of the various parts of the system. In the third part and to validate our model, examples of simulation results using Matlab/Simulink software will be presented and analyzed.

2. MODELING SYSTEM WIND VARIABLE SPEED BASED ON DFIG

The variable speed wind system studied in this article, based on a DFIG, is shown in figure 1. The turbine through a multiplier causes the DFIG, which is connected to the power grid by the stator but also through three-phase IGBT static converters by the rotor. These converters, later in this paper, are controlled by Pulse Width Modulation (PWM) [7].

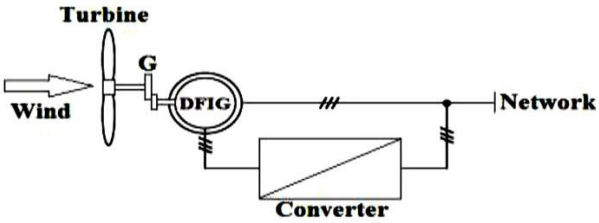

Fig. 1: Diagram of a wind energy conversion chain

2.1 Wind turbine model

2.1.1 Aerodynamic model

The wind speed, applied on the blades of the windmill, its causes rotated and creates mechanical power on the shaft of the turbine, speaking by [8, 9].

$$P_t = \frac{1}{2} C_p(\lambda,\beta).\rho.S^3 \quad (1)$$

Where λ is defined by:

$$\lambda = \frac{\Omega_t . R}{v} \quad (2)$$

C_p is the power coefficient with the theoretical limit is 0.59; λ is the specific speed; ρ the density of air (approximately 1.225 kg/m^3 à 15°C); S is the area swept by the blades; Ω_t is the rotational speed of the turbine; R is the radius of a wind turbine or the length of a blade. [8, 9].

In the context of this article, we use an approximate expression of the power coefficient as a function of the relative speed λ and the pitch angle of the blades β whose expression originates from the work [10, 11].

$$C_p(\lambda,\beta) = (0.5 - 0.0167\times(\beta - 2))\times\sin\left(\frac{\pi(\lambda + 0.1}{10-0.3\times\beta}\right) - 0.00184\times(\lambda - 3)\times(\beta - 2) \quad (3)$$

Expression of the aerodynamic torque is given by:

$$C_t = \frac{P_t}{\Omega_t} + \frac{\pi}{2\lambda}\rho.R^3.C_p(\lambda,\beta) \quad (4)$$

2.1.2 Model of the mechanical part

It is considered that the mechanical system is characterized by the sum of all the mechanical characteristics; we obtain a mechanical model with two masses (figure 2).

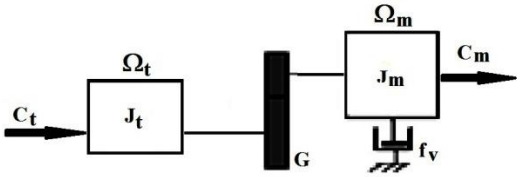

Fig. 2: Mechanical model of the wind turbine

The machine is suitable to the turbine via a speed multiplier gain G as shown in figure 2. The resulting equations are given by (5) and (6).

J_t, Moment of inertia of the turbine; J_m, Moment of inertia of the DFIG; f_v, Viscous friction coefficient of the DFIG, C_m, Mechanical torque on the shaft of the DFIG.

$$C_m = C_t / G \quad (5)$$

$$\Omega_m = G \times \Omega_t \quad (6)$$

According to figure 3, we can write the fundamental equation of the dynamics of the mechanical system on the mechanical tree of DFIG by:

$$\left(\frac{J_t}{G^2} + J_m\right)\frac{d\Omega_m}{dt} + f_v.\Omega_m = C_m - C_{em} \quad (7)$$

C_{em}, The electromagnetic torque of the DFIG.

The block diagram of figure 3 corresponds to the aerodynamic and mechanical modeling of the wind turbine [9].

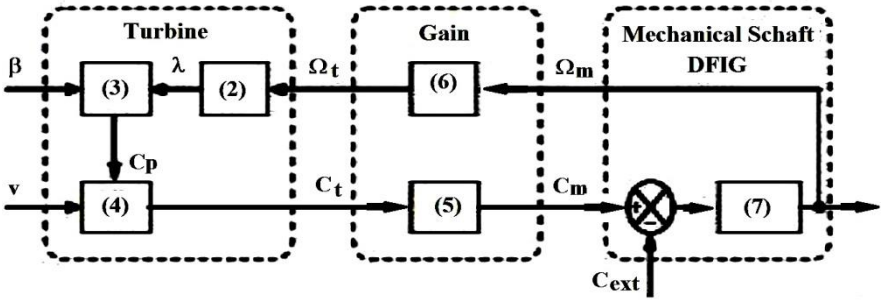

Fig. 3: Modeling of the mechanical part of the wind turbine

2.2 Modeling of DFIG

In order to establish vector control of MADA, we remind here the modeling in the landmark Park.

The model is based on the following standard simplifying assumptions [12]:

- Constant air gap,
- Effect of neglected notches,
- Sinusoidal spatial distribution of gap magnetomotive forces,
- Influence of the skin effect and of the non-addressed heating,
- Unsaturated magnetic circuit and constant permeability,
- No zero sequence regime since the neutral is not connected.

The equation for the stator and rotor of the tensions in the reference of DFIG Park are defined by [9].

$$V_{sd} = R_s . I_{sd} + \frac{d\varphi_{sd}}{dt} - \omega_s \varphi_{sq} \quad (8)$$

$$V_{sq} = R_s . I_{sq} + \frac{d\varphi_{sq}}{dt} + \omega_s \varphi_{sd} \quad (9)$$

$$V_{rd} = R_r . I_{rd} + \frac{d\varphi_{rd}}{dt} - \omega_r \varphi_{rq} \quad (10)$$

$$V_{rq} = R_r . I_{rq} + \frac{d\varphi_{rq}}{dt} + \omega_r \varphi_{rd} \quad (11)$$

V_{sd}, V_{sq}, the stator voltages in the reference Park, V_{rd}, V_{rq}, the rotor voltages in the reference Park, I_{sd}, I_{sq}, the stator currents in the reference Park, I_{rd}, I_{rq}, the stator currents in the reference Park, $\varphi_{sd}, \varphi_{sq}$, the stator flux in the reference Park, $\varphi_{rd}, \varphi_{rq}$, the rotor flux in the reference Park, R_S, R_r, the reristance of the stator and rotor windings.

The stator and rotor flux are expressed by [9]:

$$\varphi_{sd} = L_s . I_{sd} + M . I_{rd} \quad (12)$$

$$\varphi_{sq} = L_s . I_{sq} + M . I_{rq} \quad (13)$$

$$\varphi_{rd} = L_r . I_{rd} + M . I_{sd} \quad (14)$$

$$\varphi_{rq} = L_r . I_{rq} + M . I_{rq} \quad (15)$$

L_s, the cyclic stator inductance; L_r, the cyclic rotor inductance; M, the magnetizing inductance.

The electromagnetic torque C_{em} is expressed by:

$$C_{em} = p \frac{M}{L_s} (\varphi_{sd} \cdot I_{rq} - \varphi_{sq} . I_{rd}) \quad (16)$$

P, Number of pole pairs

The active and reactive power stator and rotor are expressed by:

$$P_s = V_{sd} . I_{sd} + V_{sq} . I_{sq} \quad (17)$$

$$Q_s = V_{sq} . I_{sd} - V_{sd} . I_{sq} \quad (18)$$

$$P_r = V_{rd} . I_{rd} + V_{rq} . I_{rq} \quad (19)$$

$$Q_r = V_{rq}.I_{rd} - V_{rd}.I_{rq} \quad (20)$$

The frequency of the stator voltage being imposed by the electric network, the pulsating current is rotriques:

$$\omega_r = \omega_s - P\,.\,\Omega \quad (21)$$

ω_r and ω_s, stator and rotor pulsation (rad/s)

2.3 Modelling of the three-phase inverter

The general structure of a three-phase voltage of two-level inverter is shown in figure 4. It consists of two switches (IGBT) by arms [13].

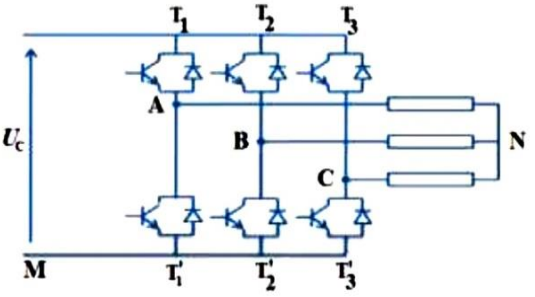

Fig. 4: Three-phase voltage inverter

The state of the switches, assumed perfect, can be represented by three Boole and control variables S_j ($j=\{a,b,c\}$), such that:

$S_j = 1$ If T_i $(i = \{1,2,3\})$ is closed and T_i' is open.

$S_j = 0$ If T_i $(i = \{1,2,3\})$ is open and T_i' is closed.

The objective of the modeling is to find a relationship between the controlled variables and the electrical variables of the alternative portion and continues to the inverter. The output voltages of the inverter are expressed by [14]:

$$\begin{bmatrix} V_{An} \\ V_{Bn} \\ V_{Cn} \end{bmatrix} = \frac{U_c}{3} \begin{bmatrix} 2 & -1 & -1 \\ -1 & 2 & -1 \\ -1 & -1 & 2 \end{bmatrix} \times \begin{bmatrix} S_a \\ S_b \\ S_c \end{bmatrix} \quad (22)$$

In our work, the control of the switch of the inverter is achieved by the use of the PWM control (pulse width modulation).

3. CONTROL STRATEGIES WIND SPEED VARIABLE SYSTEM BASED ON DFIG

The overall strategy control system comprises: control generator speed control power (active and reactive) from the inverter connected to the rotor of the machine.

3.1 Control strategy of the speed of the generator

For the speed control of the DFIG, one must adjust the electromagnetic torque on the shaft of the DFIG so as to fix the rotational speed there of to a reference speed as shown in figure 5 [9].

The references electromagnetic torque C_{em}^{*} for obtaining a rotational speeds Ω_m equal to its reference value Ω_m^{*} is obtained at the output of the speed controller ('Reg speeds' in figure 5. The regulator of the type Proportional Integral,

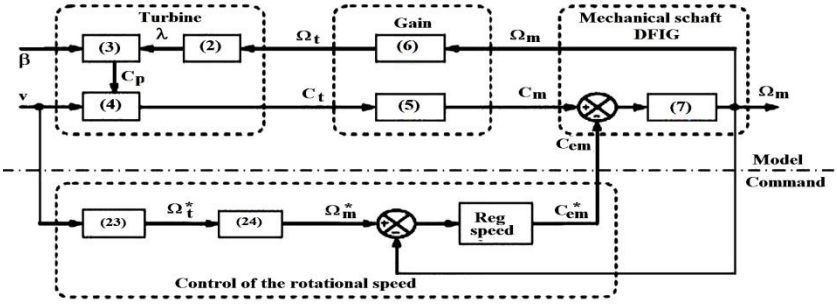

Fig. 5: Principle of speed control of the generator

The reference rotation speed Ω_t^{*} of the turbine is obtained from equation (2) and is defined by:

$$\Omega_t^{*} = \frac{\lambda_{opt}.v}{R} \tag{23}$$

We deduce the DFIG rotational speed reference taking into account the gain of the multiplier by:

$$\Omega_m^{*} = G\,.\,\Omega_t^{*} \tag{24}$$

3.2 Strategy for control of active power and reactive

In this paper, we proposed a vector control law for DFIG based on the orientation of the stator flux. The latter shows the relationship between the stator and the rotor variables. These relationships will enable the rotor to act on signals to control the exchange of real and reactive power between the stator of the machine and the network.

In this command, the stator flux is oriented along the axis. Thus, we can write [12]:

$$\begin{cases} \varphi_{sd} = \varphi_s \\ \varphi_{sq} = 0 \end{cases} \tag{25}$$

The expression of the electromagnetic torque becomes:

$$C_{em} = p.\frac{M}{L_s}.I_{rq}.\varphi_{sd} \tag{26}$$

If the stator resistance R is neglected, which is a realistic assumption for high power generators used in wind systems [9, 15] simplifying the equations of DFIG in the dq reference can be obtained from equations (8 and 9):

$$V_{sd} = 0 \tag{27}$$

$$V_{sq} = V_s = \omega_s \varphi_s \tag{28}$$

From equations (12) and (13), we obtain the following expressions stator currents:

$$I_{sd} = -\frac{M}{L_s} I_{rd} + \frac{\varphi_s}{L_s} \tag{29}$$

$$I_{sq} = -\frac{M}{L_s} I_{rq} \tag{30}$$

According to equations (26), (27), the active and reactive powers stator is written:

$$P_s = V_s . I_{sq} \tag{31}$$

$$Q_s = V_s . I_{sd} \tag{32}$$

For the expression of power in function of the rotor currents, is replaced in the above equation the current by the equations (28), (29):

$$P_s = -V_s . \frac{M}{L_s} . I_{rq} \tag{33}$$

$$Q_s = -V_s . \frac{M}{L_s} . I_{rd} + V_s . \frac{\varphi_s}{L_s} \tag{34}$$

From the expressions (26), (27), we obtain for the stator flux, the following expression:

$$P_s = -V_s . \frac{M}{L_s} . I_{rq} \tag{35}$$

$$Q_s = -V_s . \frac{M}{L_s} . I_{rd} + \frac{V_s^2}{L_s . \omega_s} \tag{36}$$

Substituting in equations (14), (15), the stator currents by the expressions (28), (29) we obtain:

$$\varphi_{rd} = \left(L_r - \frac{M^2}{L_s} \right) . I_{rd} + \frac{M . V_s}{L_s . \omega_s} \tag{37}$$

$$\varphi_{rq} = \left(L_r - \frac{M^2}{L_s} \right) . I_{rq} \tag{38}$$

From these equations, one can deduce the expressions of rotor voltages:

$$V_{rd} = R_r . I_{rd} + \left(L_r - \frac{M^2}{L_s} \right) . \frac{d I_{rd}}{d t} - \omega_r . \left(L_r - \frac{M^2}{L_s} \right) I_{rq} \tag{39}$$

$$V_{rq} = R_r . I_{rq} + \left(L_r - \frac{M^2}{L_s} \right) . \frac{d I_{rq}}{d t} + \omega_r . \left(L_r - \frac{M^2}{L_s} \right) I_{rd} + \omega_r . \frac{M}{L_s} . \varphi_s \tag{40}$$

In steady state, the terms involving derivatives of two-phase rotor currents disappear.

By combining the different equations of flows, the rotor voltages, currents and powers, we can express the tensions depending on power. Thus reproducing the system

modeling the opposite direction resulting in a pattern that matches that of the machine but the other way and contains all the elements of the DFIG simplified model.

To regulate the power optimally, it will set up two control loops one ach axis with a proportional integral regulator (PI) for each, a loop for power and one for the current while compensating for interference terms and coupling of the d and q axes. We thus obtain the control structure shown in figure 6.

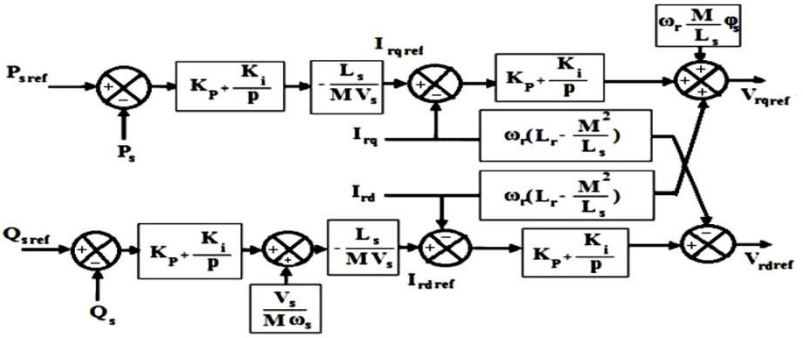

Fig. 6: Block diagram of the control structure
for orientation of the stator flux of the DFIG

The proportional integral PI controller, used to control the DFIG as a generator, is simple and quick to implement while providing acceptable performance [4, 12]. That why it caught our attention for a comprehensive study of the system.

Figure 7 shows a part of the closed loop system and corrected by a PI controller whose transfer function is of the form $k_p + k_i / p$ corresponding to controllers used in figure 6.

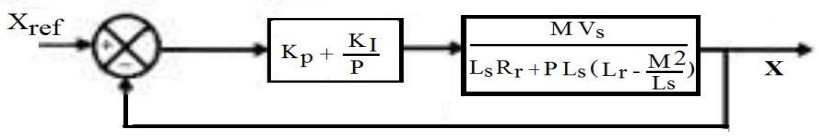

Fig. 7: Scheme of the system with feed-back loop

The Open Loop Transfer Function (FTBO) with regulators is written as follows:

$$FTBO = \frac{p+\frac{k_i}{k_p}}{\frac{p}{k_p}} \frac{\frac{MV_s}{L_s.\left(L_r-\frac{M^2}{L_s}\right)}}{p+\frac{L_s.R_r}{L_s.\left(L_r-\frac{M^2}{L_s}\right)}} \tag{41}$$

We choose the pole compensation method for the synthesis of the regulator to eliminate the zero of the transfer function. This leads to the following equality:

$$\frac{k_i}{k_p} = \frac{L_s . R_r}{L_s . \left(L_r - \frac{M^2}{L_s} \right)} \tag{42}$$

If it clears, we obtain the following FTBO

$$FTBO = \frac{k_p . \frac{M V_s}{L_s . \left(L_r - \frac{M^2}{L_s} \right)}}{p} \tag{43}$$

This give us a closed loop:

$$FTBT = \frac{1}{1 + p \tau_r} \quad \text{with} \quad \tau_r = \frac{1}{k_p} \frac{L_s . \left(L_r - \frac{M^2}{L_s} \right)}{M . V_s} \tag{44}$$

We can now express the gains correctors according to the parameters of the machine and response time:

$$k_p = \frac{1}{\tau_r} \frac{L_s . \left(L_r - \frac{M^2}{L_s} \right)}{M . V_s} \; ; \; k_i = \frac{1}{\tau_r} \frac{R_r . L_s}{M . V_s} \tag{45}$$

4. SIMULATION OF WIND CHAIN

The simulation was performed with the Matlab/Simulink software to validate investigated orders.

We made two points of operation, a variable speed with asynchronous step hypo and hyper synchronous fashion and the other with variable speed wind turbine (Variable wind profile). The wind speed is modeled by a deterministic form sum of several harmonics [3, 16]:

$$v = v_0 + \sum_{i=1}^{n} A_i \sin(\omega_i t + \varphi_i) \tag{46}$$

An example of wind profile constructed from the spectral characteristic of Van der Hoven and this profile that will be applied to the system studied in this article. His equation is given by [3, 16]:

$$\begin{aligned} v = 12 &+ 2\sin(2.5t - \frac{\pi}{5}) + 2\sin(4t - \frac{\pi}{3}) \\ &+ 1.5\sin(5.4t - \frac{\pi}{12}) + 0.5\sin(2.5t - \frac{\pi}{12}) \end{aligned} \tag{47}$$

4.1 Wind energy system control by a speed step

We put the system of 0s – 5s hyper synchronous mode 250 rad/s and of 5s – 10s hypo synchronous 150 rad/s shown in the figure 8.

Figure 9 is figure 10 shows the simulation results obtained by the indirect control of power generated at the stator of the DFIG. The command decouples the expressions of active and reactive power of the generator or the one of the flux and torque. We find that the reference variables were monitored by DFIG for both active and reactive power.

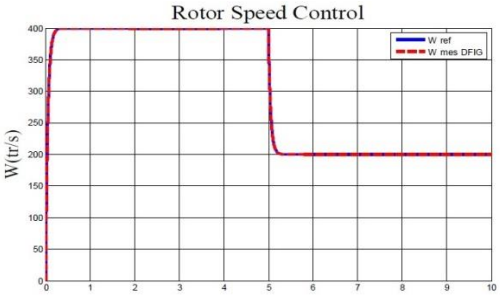

Fig. 8: Rotation speed DFIG

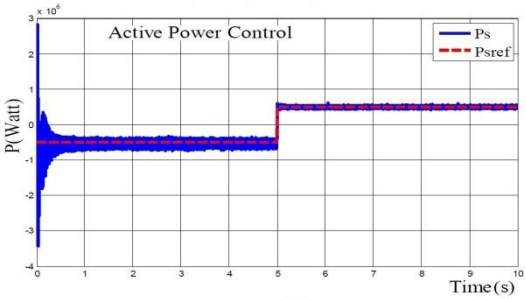

Fig. 9: Stator active power

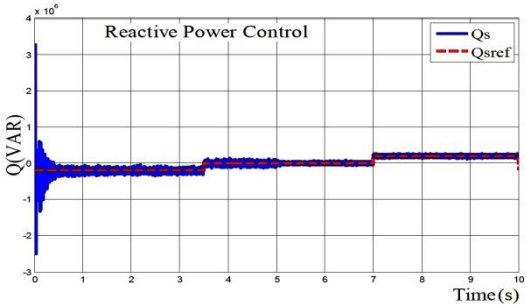

Fig. 10: Stator reactive power

4.2 Wind system control by variable speed wind turbine (variable wind profile)

Figure 11 shows the shape of the speed vent. Figure 12 shows the total mechanical power of the turbine. The result of the mechanical speed control is presented in figure 13. These curves show that the proposed control strategy is satisfactory, that is to say the measured speed is identical to the reference obtained. The active power measured in the stator of the DFIG is presented in figure 14.

The measured active power shows good agreement with that of the reference which is set at 40 % of the total mechanical power. In addition, figure 14 shows that the control strategy takes into account the variations of the wind speed. The reference reactive power is set to −2MVAr between 0s and 3.5s; 0MVAr between 3.5s and 7s; then 2MVAr

between 7s and10s. The reactive power control result is shown in figure 15 where the reference power and that measured have a good agreement.

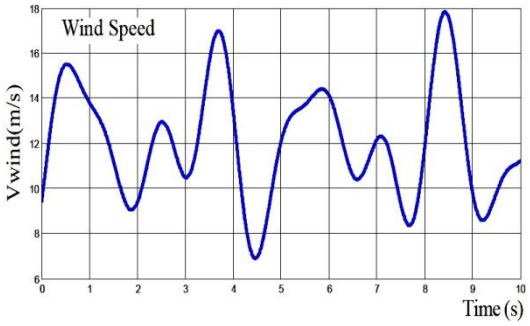

Fig. 11: Wind speed

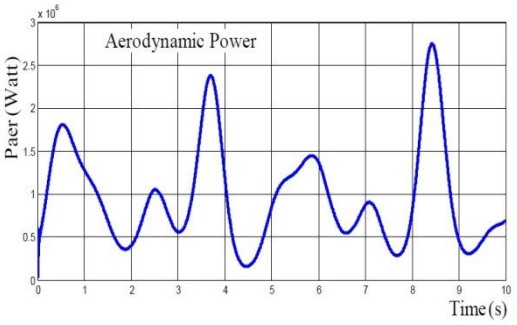

Fig. 12: Total mechanical power of the turbine

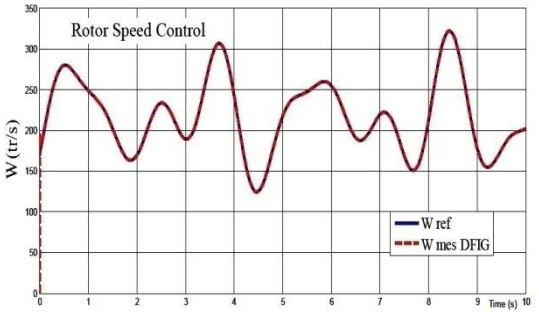

Fig. 13: Rotation speed DFIG

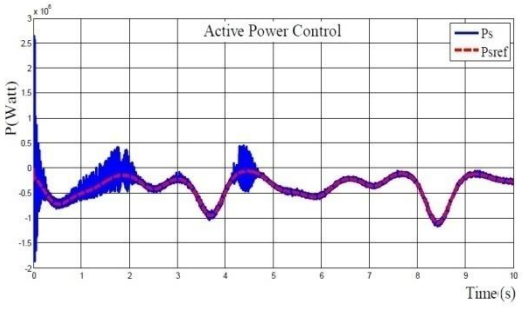

Fig. 14: Stator active power

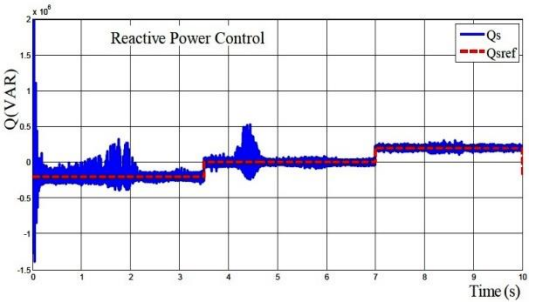

Fig. 15: Stator reactive power

5 CONCLUSION

This article was dedicated to the modeling, the simulation and the analysis of a wind turbine operating in variable speed based on DFIG. First, we are interested in modeling different parts of the wind turbine system, and then two control strategies of the wind energy system have been detailed. The speed of the generator control strategy can provide all of the active power produced to the electricity grid with a unity power factor. However, decoupled control of active and reactive power with the application of the flow direction control makes stable wind system and helps regulate active and reactive power supplied to the network according to defined by the network operator instructions. Finally, simulation results of the command of the complete wind system by both strategies were presented to validate the performance of the control techniques used.

APPENDIXES

Table 1: Turbine parameter's [11]

Parameter's	Value
Rated power	1.5 MW
Radius of the wind	35.25 m
Gearbox ratio	90

Table 2: DFIG parameter's [11]

Parameter's	Value
Rated power	1.5 MW
Stator voltage	690 V
Stator frequency	50 Hz
Stator resistance	0.012 Ohm
Rotor resistance	0.021 Ohm
Stator inductance	0.0137 H
Rotor inductance	0.0136 H
Mutual resistance	0.0135 H
Moment of inertia	1000 kg.m^2
Coefficient of friction	0.0024 kg. m^2/S
Numbers of pole pairs	2

Table 3: PI controller parameter's

Parameter's	Value
Control parameter's of the speed of DFIG	$k_p = 1.64\times10^5$; $k_i = 1.3456\times10^7$
Control parameter's of the rotor currents	$k_p = 0.0363$; $k_i = 2.5632$
Control parameter's of the active and reactive power	$k_p = 200$; $k_i = 1$

REFERENCES

[1] O. Gergaud, '*Modélisation Energétique et Optimisation Economique d'un Système de Production Eolien et Photovoltaïque Couplé Au Réseau et Associé à un Accumulateur*', Thèse de Doctorat, Ecole Normale Supérieure de Cachan, France, 2002.

[2] F. Poitiers, M. Machmoum, R. Le Doeuff and M.E. Zaim, '*Control of a Doubly-Fed Induction Generator for Wind Energy Conversion Systems*', International Journal of Renewable Energy Engineering, Vol. 3, N°3, pp. 373 – 378, 2001.

[3] A.Y. Sylla, '*Modélisation d'un Emulateur Eolien à Base de Machine Asynchrone a Double Alimentation*', Mémoire de l'Université du Quebec, aux Trois-Rivières, 2013.

[4] F. Poitiers, '*Etude et Commande de Génératrices Asynchrones pour l'Utilisation de l'Energie Eolienne: Machine Asynchrone à Cage Autonome, Machine Asynchrone à Double Alimentation Reliée au Réseau*', Thèse de Doctorat, Ecole Polytechnique de l'Université de Nantes, France, 2003.

[5] R. Defontaines, '*Etude et Simulation de la MADA*', Mémoire de Maîtrise Electronique, Ecole de Technologie Supérieure, Montreal, Juin 2012.

[6] C. Belfedal, S. Moreau, G. Champenois, T. Allaoui and M. Deni, '*Comparison of PI and Direct Power Control with SVM of Doubly Fed Induction Generator*', Istanbul University, Journal of Electrical & Electronics Energineering, Vol.8, N°4, pp. 663 - 641, 2008.

[7] J.A. Baroudi, V. Dinavahi and A.M. Knight, '*A Review of Power Converter Topologies for Wind Generators*', Renewable Energy, Vol. 32, N°14, pp. 2369 - 2385, 2007.

[8] S. Heier, '*Grid Integration of Wind Energy Conversion Systems*', John Wiley & Sons, 1998.

[9] A. Gaillared, '*Système Eolien basé sur une MADA: Contribution à l'Etude de la Qualité de l'Energie Electrique et de la Continuité de Service*', Thèse de Doctorat, Université Henri Poincaré, Nancy1, 2010.

[10] S. El aimani, B. Francois, B. Robyns and F. Minne, 'Modeling and Simulation of Doubly Fed Induction Generators for Variable Speed Wind Turbines Integrated in a Distribution Network', 10th European Conference on Power Electronics and Applications (EPE 2003), Toulouse, France, September 2003.

[11] S. El Aimani, '*Modélisation de Différentes Technologies d'Eoliennes Intégrées dans un Réseau de Moyenne Tension*', PhD Thesis, Ecole Centrale de Lille, 2004.

[12] P.E. Vidal, '*Commande non-Linéaire d'une Machine Asynchrone à Double Alimentation*', Thèse de Doctorat, en Génie Electrique, Institut National Polytechnique, Toulouse, 2004.

[13] B. Robyns and P. Bastard, '*Production Décentralisée d'Electricité: Contexte et Enjeux Techniques*', 3EI Review, N°39, pp. 5 – 13, Décembre 2004,

[14] C.C. de Wit, '*Modélisation, Contrôle Vectoriel et DTC*', Paris, Hermes Science Publications, 2000.

[15] S. Muller, M. Deicke and R.W. de Doncker, '*Doubly Fed Induction Generator Systems for Wind Turbines*', IEEE Industry Applications Magazine, Vol. 8, N°3, pp. 26 - 33, May-June 2002.

[16] Y. Liu and J. Wang, '*A Large Time Scale Wind Velocity Simulation Method*', in International Conference on Computer Design and Applications (ICCDA), 2010, pp. V4-282 - V4-286, 2010.